Efficient Blue-Light-Emitting Polymer Heterostructure Devices: The Fabrication of Multilayer Structures from Orthogonal Solvents

By *Stefan Sax, Nicole Rugen-Penkalla, Alfred Neuhold, Sebastian Schuh, Egbert Zojer, Emil J. W. List,** and *Klaus Müllen**

The development of the first polymer light-emitting device (PLED) by Burroughes et al. in 1990[1] had a tremendous impact on industrial as well as scientific research due to the potential applications of PLEDs in large-area display[2] or solid-state lighting applications.[3,4]

For both implementations, color-stable and efficient electroluminescent devices in the red, green, and blue spectral range are needed. To achieve the targeted lifetime beyond ten thousand of hours, several requirements must be met such as chemical stability of the active materials as well as very low concentrations of chemical defects and other impurities. Stable green- and red-emitting polymers are already well established, whereas stable blue-emitting materials and corresponding optimized device structures are still under development. Due to the relatively low sensitivity of the human eye in the blue wavelength range, those devices require a higher power consumption to achieve equal luminous values.

A basic design feature generally used in inorganic as well as organic solid-state semiconductor devices is the so called heterostructure, combining semiconductors with different bandgaps, band offsets and/or transport properties to yield enhanced device performance. So far, various approaches towards heterostructure device architectures enhancing the efficiency have been demonstrated for organic solid-state devices. Auxiliary injection layers,[5] doped interface regions,[6] or multiple tandem structures comprising Cs_2CO_3/MoO_3 interconnecting layers[7] have been used to enhance and balance charge injection and transport as well as exciton formation in the device. Moreover, molecularly doped n and p regions can be implemented, allowing the transfer of many successful design principles of inorganic semiconductor physics to organic semiconductors.[8]

[*] Prof. E. J. W. List, Dr. S. Sax, A. Neuhold
NanoTecCenter Weiz Forschungsgesellschaft mbH
Franz-Pichler-Straße 32, A-8160 Weiz (Austria)
E-mail: list@ntc-weiz.at
Prof. K. Müllen, N. Rugen-Penkalla
Max Planck Institute for Polymer Research
Ackermannweg 10, D-55128 Mainz (Germany)
E-mail: muellen@mpip-mainz.mpg.de
Prof. S. Schuh, Prof. E. Zojer, E. J. W. List
Institute of Solid State Physics
Graz University of Technology
Petersgasse 16, A-8010 Graz (Austria)

DOI: 10.1002/adma.200903076

In contrast to polymer based devices, such multilayer heterostructures can simply be realized with small molecules by using various thermal vacuum deposition techniques. Although small molecules can be solution processed, multilayer organic light-emitting diode (OLED)-structure preparation is also hampered by resolvation of the subsequent layer. Within the scope of industrial mass production, organic light-emitting devices based on the thermally evaporated small molecules suffer from the high-vacuum deposition process steps, which clearly limit the size of the targeted application. Alternatively, large-area applications can be easily realized from solution-based processable organic semiconductors (small molecules or polymers) allowing for cost-effective printing processing techniques[9] and roll-to-roll fabrication. Yet, the crucial issue of solution-based multilayer PLEDs is not to dissolve or "harm" already prepared layers by the solvent used in subsequent deposition process. Various approaches have been suggested so far, ranging from liquid buffer layers between the individual polymer layers[10] to in situ converted or crosslinked electro-optical active polymer layers.[11–14] Moreover, Ma et al. showed that a water/methanol soluble conjugated copolymer with ionic side chains coated on top of a light-emitting layer can act as electron-transport and injection layer in a PLED.[15] However, polymers containing ionic side chains also show intrinsic electrochemical doping, at least at one polymer/electrode interface.[16] All above approaches do have their merits; still, in many cases device efficiency is traded in for long-term stability due to potential defects introduced in the active material and/or device structure.

To overcome these issues, here, we present a novel processing strategy to establish multilayer hetero device structures, which i) does not alter the intrinsic properties of the utilized semiconductors and ii) does not introduce any additional potential electronic defects into the material and the device structure. To that aim, the solubility of polyfluorenes in organic solvents of different polarity is adequately tuned: when substituting alkyl side chains by ethylene glycol side chains of appropriate length we can successfully suppress re-dissolving and intermixing during subsequent spin-coating processes in the device fabrication without the use of crosslinking agents, buffer layers, or ionic side chains. Moreover, as will be shown here, using a combination of two properly chosen blue-emitting polymeric semiconductors to build heterostructure devices along the lines described above, remarkable improvements in device efficiency can be achieved. This is attributed to enhanced exciton formation as a consequence of efficient hole blocking at the polymer/polymer heterodevice interface.

In this study, a new methanol-soluble polyfluorene with nonionic side chains is reported, where different ethylene glycol oligomers are introduced at the 9-position of the fluorene. This new polymer is designed such that the side chains afford, firstly, a good solubility, secondly, a high polarity, and, thirdly, a satisfying molecular weight. Due to the fact that too short polar side chains do not provide enough polarity, whereas too long substituents hinder polymerization, fluorene monomers with methoxytetra-(ethylene glycol) **2** as well as methoxypoly(ethylene glycol) chains **3** were used (Fig. 1). A statistical copolymerization of monomer **2** and **3** via Yamamoto reaction would not ensure the same ratio of **2** and **3** and thus a defined solubility. Therefore, the polymerization was performed via Suzuki coupling of the bisboronic ester **4** and the dibromo macromonomer **3**, since this reaction guarantees an alternating substitution pattern. As desired, the obtained poly[9,9-bis(methoxytetra(ethylene glycolyl)-2,7-fluorene)-*alt*-(9,9-bis(methoxypoly(ethylene glycolyl)-2,7-fluorene)] **5** (further called PF_{polar}) shows high solubility in methanol and ethanol in contrast to PFs carrying short polar side chains as reported earlier.[17] Hence, this PF_{polar} provides the opportunity to study heterostructure PLED systems, processed via sequential spin-coating, using orthogonal solvents, since most commonly used conjugated polymers with alkyl side chains are insoluble in methanol and ethanol.

In order to attain deep-blue-light-emitting heterostructure PLEDs both active materials must provide sufficient bandgaps to yield blue emission. Hence, as the appropriate active material for the first layer (below the PF_{polar}) a poly(tetraarylindenofluorene)[18] (PIF) has been selected. The optical bandgaps of the two materials differ by ca. 90 meV as determined from the onset of the absorption.[18,19] Both polymers are well studied and behave very similarly in terms of their optical and electrical properties, making them ideal model materials to study heterostructure device physics. Moreover, as confirmed by quantum-chemical calculations, an asymmetric shift of the lowest unoccupied molecular orbital (LUMO) and highest occupied molecular orbital (HOMO) energy levels at the polymer/polymer interface occurs (see below and the Supporting Information), which results in a type-1 band alignment (i.e., no exciton dissociation is taking place, such as in a solar cell) and in a considerable larger barrier for holes than for electrons at the PIF/PF_{polar} interface.

A typical device comprises a glass substrate covered with a 120-nm-thick indium tin oxide (ITO) layer acting as anode, followed by a 90-nm-layer of poly(3,4-ethylenedioxythiophene)–polystyrenesulfonic acid (PEDOT:PPS). The active layer of the investigated devices consists of either of one of the two polymers or of a bilayer. Finally, a 4-nm-thick caesium fluoride (CsF) layer covered with a 100-nm-aluminium layer was evaporated on top, acting as the cathode. Before fabricating heterostructure devices extensive studies on film formation have been performed. To determine a possible reduction of film thickness due to resolvation of the PIF-layer by the PF_{polar}/ethanol solution during spin coating, a PIF film was treated with pure ethanol. Atomic force microscopy (AFM) confirmed the stability of PIF against ethanol, finding no change in the actual layer thickness before and after treatment and no significant increase of the RMS roughness.

In Figure 2a and 2b the device characteristic for ITO/PEDOT:PSS/Polymer/CsF/Al-PLED structures are shown for PIF and PF_{polar}, respectively. Both devices are optimised for efficiency with respect to the active-layer film thickness. PIF shows a bright deep-blue electroluminescence spectrum (Commission Internationale de l'Eclairage (CIE): $x = 0.18$; $y = 0.16$) with a maximum at 2.87 eV (432 nm) and a shape identical to the photoluminescence emission spectrum of the solid state film. Luminance values of typically 850 cd m^{-2} can be found at 10 V bias. The devices demonstrate remarkable spectral stability over time as reported earlier.[18] The devices display an electroluminescence (EL) onset at ca. 3.8 V with a maximum efficiency of ca. 0.25 cd A^{-1}. PF_{polar} also exhibit bright deep-blue stable EL spectra CIE: $x = 0.19$; $y = 0.20$) with a maximum at 2.93 eV (423 nm) and an EL onset at 3.2 V. Luminance values of typically 400 cdm^{-2} are found at 10 V bias, yielding a device efficiency of ca. 0.06 cd A^{-1}. An evaluation of the EL spectrum shows that the exchange of the side chains from nonpolar alkyl chains (as typically used for such polymers) to ethylene glycol type side chains does not significantly alter the optical properties of the polymer.[19]

As depicted in Figure 2c, the best heterostructure device comprising a 22-nm PF_{polar} layer on top of a 55-nm PIF active layer in a ITO/PEDOT:PSS/PIF/PF_{polar}/CsF/Al-PLED architecture shows the bright deep-blue emission of PIF with a maximum at 2.86 eV (433 nm; CIE coordinates at $x = 0.21$; $y = 0.21$) with an EL onset at ca. 3.4 V. For optimising the device performance the thickness of both active polymer layers has been varied in the range between 20 nm and 60 nm. Such optimised hetero-structured PIF-PF_{polar} devices exhibit a maximum luminance of 1400 cd m^{-2} at 10 V bias. The devices show a remarkable efficiency of 1.23 cd A^{-1}. This

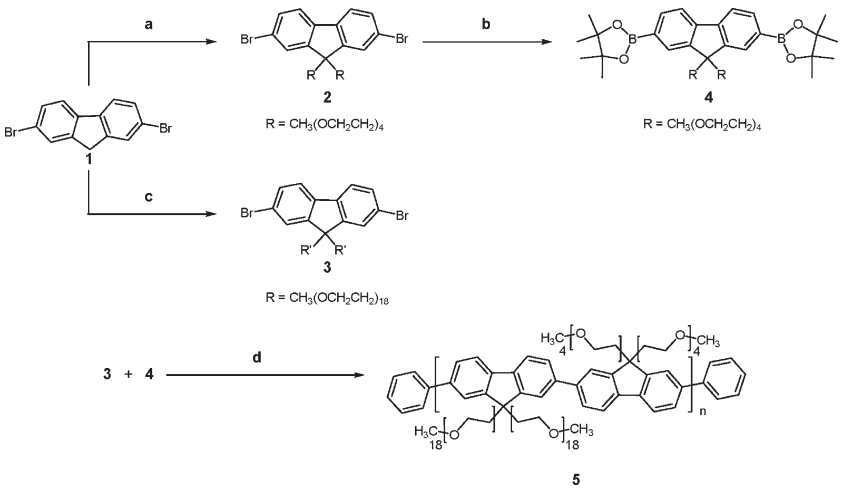

Figure 1. Synthesis of the methanol-soluble polyfluorene 5. a) Anhydrous dimethylformamide (DMF), NaH, $CH_3(OCH_2CH_2)_4OTs$ (OTs = tosylate), room temperature (r.t.), 91%. b) Anhydrous 1,4-dioxane, bispinacolatodiboron, KOAc (OAc = acetate), $PdCl_2(dppf)$, 80 °C, 44%. c) Anhydrous DMF, NaH, $CH_3(OCH_2CH_2)_{18}Br$, r.t., 90%. d) $Pd(PPh_3)_4$, 1,4-dioxane, 1 M $NaHCO_3$, bromobenzene, phenyl boronic acid, 90 °C, 78%.

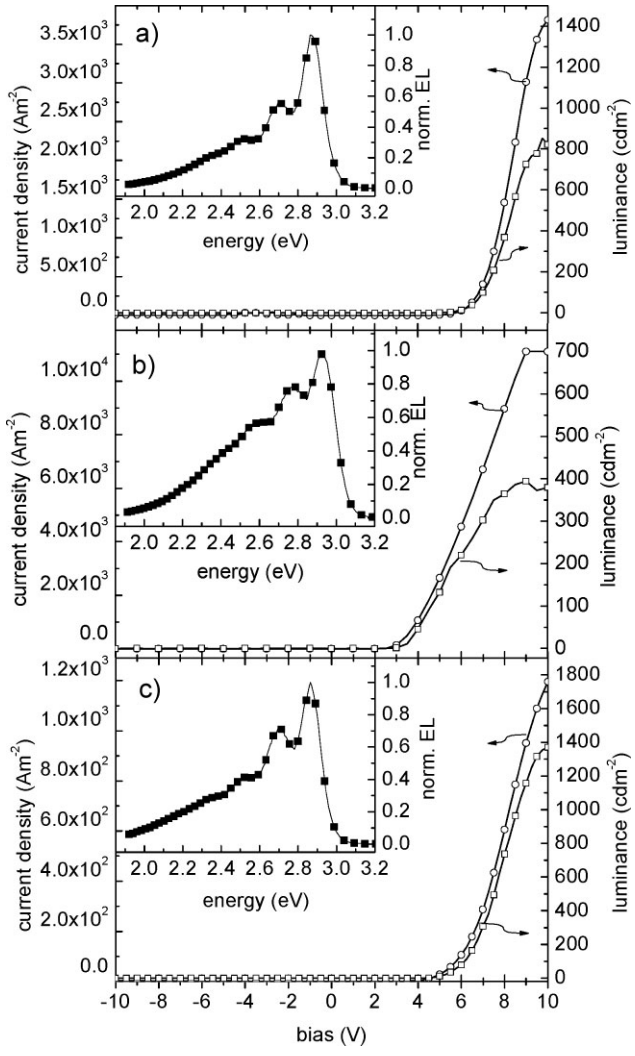

Figure 2. a) Current density and luminance as a function of the bias voltage in an ITO/PEDOT:PSS (90 nm)/PIF (55 nm)/CsF (4 nm)/Al (100 nm) device. The inset shows the normalized EL spectrum of the device with CIE coordinates of $x = 0.18$; $y = 0.16$. A maximum device efficiency of 0.25 cd A^{-1} was found. b) Current density and luminance as a function of the bias voltage in an ITO/PEDOT:PSS (90 nm)/PF$_{polar}$ (22 nm)/CsF (5 nm)/Al (100 nm) device. The inset shows the normalized EL spectrum of the device with CIE coordinates of $x = 0.19$; $y = 0.20$. A maximum device efficiency of 0.06 cd A^{-1} was found. c) Current density and luminance as a function of the bias voltage in an ITO/PEDOT:PSS (90 nm)/PIF (55 nm)/PF$_{polar}$ (22 nm)/CsF (4 nm)/Al (100 nm) device. The inset shows the normalized EL spectrum of the device with CIE coordinates of $x = 0.21$; $y = 0.21$. A maximum device efficiency of 1.23 cd A^{-1} was found.

corresponds to a 5-fold increase compared to single-layer PIF devices and to a 20-fold increase compared to PF$_{polar}$ single-layer devices.

To explain the significant enhancement in device efficiency let us evoke the energy-level diagram of the heterostructure device as depicted in Figure 3 for a ITO/PEDOT:PSS/PIF/PF$_{polar}$/CsF PLED architecture. Considering the only minor differences in the optical bandgaps, between PF$_{polar}$ and PIF, one might expect only a very small band offset that could contribute to hole blocking; for

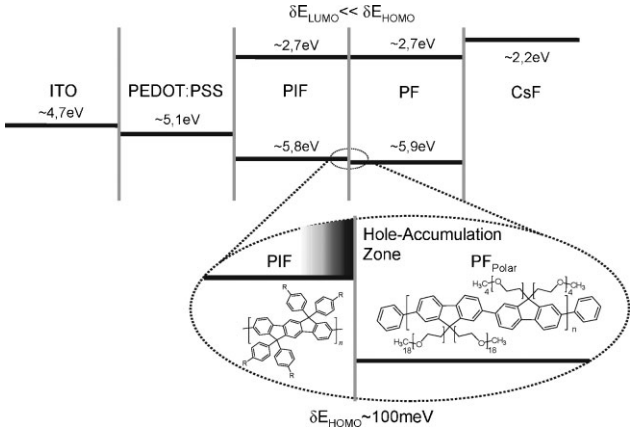

Figure 3. Schematic diagram of the energy levels (Ref. [23]) of the multilayer device structure and the chemical structure of the utilized polymers. The magnified region shows the asymmetric shift of the HOMOs as obtained from quantum-chemical calculations.

the type 1 band alignment at the PIF/PF$_{polar}$ interface, no electron blocking occurs for a device with a layer structure as shown in Figure 3. Such a situation could also offer the possibility for an energy transfer of excitons from the PF$_{polar}$ to the PIF layer in the device. In order to rule out such a process devices comprising PF$_{polar}$ doped with 1 and 3 wt% of PIF have been fabricated. However, the emission spectra of PF$_{polar}$-PIF host–guest systems are very similar to those found for devices comprising only PF$_{polar}$ and secondly typical device efficiencies are only in the range of 0.06 cd A^{-1}. Both observations rule out efficient exciton trapping as the origin for our observations. Interestingly, however, a strong asymmetry in the offsets between the HOMO and LUMO levels in the PF$_{polar}$ and PIF layers is predicted by quantum-chemical calculations using the Gaussian program suite.[20] This is consistently found independent of whether calculating orbital energies or more appropriately ionization potentials using semiempirical methods (AM1[21] in the present case) or density functional theory (DFT; here: the B3LYP functional[22] with a 6-31G(d,p) basis). All methods give rise to an additional, reasonably large hole-blocking barrier in the device at the order of 0.11 eV to 0.14 eV, depending on the used method and calculated quantity. (Obtained data are summarized in the Supporting Information). The reason for that asymmetry can be identified by studying a series of carefully chosen test molecules: Starting from a *para*-phenylene-based system, it turns out that a planarization of the backbone (as induced by the bridges in PF and more efficiently in PIF) results in a symmetric stabilization of the LUMO and destabilization of the HOMO. The distortion of the backbone induced by the bridge in conjunction with its electron-rich character compared to the hydrogens, however, destabilizes both the HOMO and the LUMO. As a net effect, introducing bridges in a polyphenylene significantly destabilizes the HOMO but only very weakly stabilizes the LUMO. This explains the asymmetry of the band offsets at the PIF/PF$_{polar}$ interface considering the larger relative number of bridges in the former polymer. This results in a barrier for holes, while providing almost no barrier for electrons at the interface between the semiconductors in the heterostructure device.

Final page numbers not assigned

To understand why this gives rise to an increased device efficiency, one hast o keep in mind that all presented and discussed devices comprise a very similar PEDOT:PSS anode for hole injection and a CsF interface material for electron injection. In such devices one typically finds an energy barrier of approximately 0.7 eV at the PEDOT:PSS interface for holes.[23] In turn the almost Ohmic contact between the low-work-function CsF layer and the used polymers makes it easy for electrons to be injected into the LUMO of the polymer.[24] Yet it was also found that due to the high field strength of trapped electrons at the PEDOT:PSS/polymer interface, hole injection is facilitated, leading to a better carrier balance between holes and electrons in devices.[25] Due to the additional hole barrier found at the interface of the semiconductors exciton formation in the PIF layer is facilitated, resulting in a higher device efficiency, which can very well account for the 5-fold, respectively 20-fold, increase in device efficiency. Note that also devices in a ITO/PEDOT:PSS/PF_{polar}/PIF/CsF PLED architecture have been fabricated. However, as a consequence of the absence of any blocking of holes or electrons in such a device structure no improvement in device efficiency and only moderate performance has been observed. Nevertheless the device efficiency is limited, independent of the device structure, by the quantum efficiency of the emitter layer as well as interface interactions between the low-work-function cathode material and the polymer interface.

Apart from PIF polyvinylcarbazole PVK[26,27] in a similar heterostructure device architecture (ITO/PEDOT:PSS/PIF/PVK/CsF) also shows a 3–5 fold improvement as compared to single-layer devices, whereas in the case of switched-polymer-layer devices (ITO/PEDOT:PSS/ PVK/PIF/CsF) only a moderate performance has been observed. Also in the case of devices with enhanced efficiency one could observe the device emission stemming exclusively from the PVK layer. Yet, the overall device performance in terms of brightness was inferior to the devices reported here.[28] Based on the presented promising fundamental study, in a next step we will further expand and optimize the concept introduced here. In particular the introduction of hole-transporting layers will be a necessity to further enhance charge injection at the anode and thereby balance available electrons and holes at the heterostructure interface to reach device efficiencies beyond 5 cd A^{-1} at an already reached brightness level of ca. 1500 cd m^{-2} based on this new concept.

In conclusion, we have presented a novel processing strategy to realize defect-free multilayer heterodevice structures by a controlled tuning of the polymer solubility from solvents of different polarity, allowing for subsequent spin-coating processes in the device fabrication without the use of crosslinking agents, buffer layers, or ionic side chains. For this purpose, a new PF copolymer with a mixture of short and long polar side chains was designed to ensure good solubility in methanol and ethanol as well as a satisfying molecular weight. Using this new blue-emitting polymer in a ITO/PEDOT:PSS/PIF/PF_{polar}/CsF/Al heterostructure PLED configuration significantly enhanced efficiencies as a consequence of enhanced exciton formation at the organic-semiconductor interface in the device could be observed. In the near future, the versatility of this fabrication method will be expanded introducing also solution-processed hole- and electron-transporting layers on either side of the polymer heterostructure. Moreover, the fabrication of all polymer based solar cells or photo detectors with defined interface regions will also be undertaken.

Experimental

^1H and ^{13}C NMR spectra were recorded on a Bruker AV 700 with the use of the solvent signal as internal standard. Melting points were determined on a Büchi hot-stage apparatus and are not corrected. Mass spectra were obtained on a VG Instruments ZAB 2-SE-FPD spectrometer by using field desorption (FD). Matrix-assisted laser desorption/ionization time-of-flight (MALDI-TOF) analysis was carried out using a Bruker Time-of-Flight MS Reflex III instrument and a dithranol matrix with THF as solvent. Gel permeation chromatography (GPC) was performed with PSS-SDV columns (SDV = styrol-divinylbenzol-copolymer; three columns, pore widths 500, 10^5, and 10^6 A) connected with UV–vis/refractive index (RI) detector. THF was used as solvent (concentration of the polymer = 1 g L^{-1}). The calibration was based on polystyrene and poly(*p*-phenylene) standards. UV–vis absorption spectra were measured using a Perkin-Elmer Lambda 900 spectrophotometer. The PL measurements were recorded on a SPEX Fluorolog 2 type 212 spectrofluorometer.

The synthesis of the monomers 1-(*p*-Tosylsulfonyl)-3,6,9,12-tetraoxotridecane (**1**), 2,7-Dibromo-9,9-bis-(1-{2-[2-(2-methoxy-ethoxy)-ethoxy]-ethoxy}-ethyl)-fluorene (**2**), 2,7-Dibromo-9,9-bis-(methoxypoly(ethylene glycolyl))-fluorene (**3**), and 2,7-Bis-(4,4,5,5-tetramethyl-[1,3,2]- dioxaborolan-2-yl)-9,9-bis-(1-{2-[2-(2-methoxy- ethoxy)-ethoxy]-ethoxy}-ethyl)-fluorene (**4**) can be found in detail in the Suppoting Information.

Poly[(9,9-bis(methoxytetra(ethylene glycolyl)-2,7-fluorene)-alt-(9,9-bis-(methoxypoly(ethylene glycolyl))-2,7-fluorene)] (**5**) was synthesized as follows: Monomer **3** (488 mg, 0.26 mmol) and bisboronic ester **4** (205 mg, 0.26 mmol) were dissolved in 1,4-dioxane (20 mL). After the addition of aqueous $NaHCO_3$ (10 mL, 1 M), the reaction mixture was degassed four times via the freeze-and-thaw technique. Finally, $Pd^0(PPh_3)_4$ (2.7 mg, 0.9 mol% with respect to bisboronic ester monomer) was added under argon atmosphere. The reaction mixture was stirred at 90 °C for 3 days. After cooling to room temperature an excess of bisboronic ester **4** (10 mg, 5 mol%) was added and the mixture was heated at 90 °C for another 3 days. The end groups were capped with phenyl boronic acid and bromobenzene (both 1.8 equivalents with respect to dibromo monomer). Before the addition of the second end-capping reagent, the solution was stirred at 90 °C for 12 h. After endcapping, the reaction mixture was dissolved in CH_2Cl_2 and washed with water until the filtrate had a neutral pH-value. The combined organic fractions were dried (Na_2SO_4) and filtered. Finally, the solvent was evaporated in order to obtain a concentrated solution, which was then added dropwise into hexane. The crude product was dissolved in THF and re-precipitated from hexane to remove impurities. The precipitate was filtered off and dried under reduced pressure to give the polymer **5** (544 mg, 78%). GPC (THF) $M_n = 11200$ g mol^{-1}, $M_w = 29800$ g mol^{-1}, D = 2.65 (polystyrene standards). ^1H NMR (700 MHz, CD_2Cl_2, δ): 7.86–7.78 (m, 12 H), 3.65–3.29 (m, 168 H), 3.25 (s, 4 H), 2.92 (s, 4 H), 2.58 (s, 4 H), 2.06 (s, 8 H). ^{13}C NMR (176 MHz, CD_2Cl_2, δ): 150.58, 140.87, 139.90, 127.06, 122.00, 120.61, 72.26, 72.24, 70.86, 70.79, 70.73, 70.69, 70.36, 67.43, 58.98, 51.98, 40.20.

The ITO-covered glass substrates for the PLEDs were cleaned in acetone, toluene, and isopropanol and subsequently exposed to oxygen plasma. PEDOT:PSS (Baytron P from Bayer Inc.) layers were spin-coated under ambient conditions and dried under inert atmosphere. Subsequently PIF dissolved in toluene with a concentration of 6 g L^{-1} was spin-coated on top of the PEDOT:PSS layer resulting in a film thickness of about 50 nm, which was dried at 120 °C under a dynamic vacuum less than 1×10^{-5} mbar. The PF_{polar} dissolved in ethanol with a concentration of 6 g L^{-1} leading to a layer thickness of around 22 nm on top of the subjacent PIF layer and was afterwards dried at 75 °C under a dynamic vacuum less than 1×10^{-5} mbar. All layer thicknesses were measured by atomic force microscopy (AFM, Veco Dimension V and a Nanoscope V Controller) and confirmed by X-ray reflectivity (XRR) measured with a Bruker diffractometer D8 Discover in Bragg–Brentano configuration (wavelength = 1.5406 Å). The multilayer cathode was thermally deposited in a vacuum coating unit at

base pressures less than 3×10^{-6} mbar. The luminescence–voltage (LV) measurements were performed using an integrating sphere equipped with a silicon photodiode and a computer controlled Keithley 237 Source Measurement Unit. Spectral characterization was done with a LOT-ORIEL Multispec equipped with a DB 401-UV CCD camera by Andor.

Acknowledgements

Financial support by the FFG in the framework of the Austrian Nano Initiative (Research Project DEVFAB in the Cluster 0700 – ISOTEC) and the Deutsche Forschungsgemeinschaft (SFP1355) is gratefully acknowledged. Supporting Information is available online from Wiley InterScience or from the author.

Received: September 7, 2009
Revised: November 13, 2009
Published online:

[1] J. H. Burroughes, D. D. C. Bradley, A. R. Brown, R. N. Marks, K. Mackay, R. H. Friend, P. L. Burns, A. B. Holmes, *Nature* **1990**, *347*, 539.
[2] J. H. Friend, R. W. Gymer, A. B. Holmes, J. H. Burroughes, R. N. Marks, C. Taliani, D. D. C. Bradley, D. A. DosSantos, J. L. Bredas, M. Lögdlund, W. R. Salaneck, *Nature* **1999**, *397*, 121.
[3] S. Tasch, E. J. W. List, O. Ekström, W. Graupner, G. Leising, P. Schlichting, U. Rohr, Y. Geerts, U. Scherf, K. Müllen, *Appl. Phys. Lett.* **1997**, *71*, 288.
[4] A. R. Duggal, C. M. Heller, J. J. Shiang, J. Liu, L. N. Lewis, *J. Disp. Technol* **2007**, *3*, 184,
[5] Riel, H. Vestweber, W. Riess, *Proc. SPIE* **1998**, *3281*, 240.
[6] M. Gross, D. C. Müller, H. G. Nothofer, U. Scherf, D. Neher, C. Bräuchle, K. Meerholz, *Nature*, **2000**, *405*, 661.
[7] T. W. Lee, T. Noh, B. K. Choi, M. S. Kim, D. W. Shin, J. Kido, *Appl. Phys. Lett.* **2008**, *92*, 043301.
[8] S. Reineke, F. Lindner, G. Schwartz, N. Seidler, K. Walzer, B. Lüssem, K. Leo, *Nature* **2009**, *459*, 234.
[9] S. C. Chang, J. Liu, J. Bharathan, Y. Yang, J. Onohara, J. Kido, *Adv. Mat.* **2005**, *17*, 734.
[10] S. R. Tsenga, H. F. Menga, C. H. Yehb, H. C. Laib, S. F. Horngb, H. H. Liaob, C. S. Hsuc, L. C. Lin, *Syn. Met.* **2008**, *158*, 130.
[11] N. C. Greenham, S. C. Moratti, D. D. C. Bradley, R. H. Friend, A. B. Holmes, *Nature.* **1993**, *365*, 628.
[12] C. D. Müller, A. Falcou, N. Reckefuss, M. Rojahn, V. Wiederhirn, P. Rudati, H. Frohne, O. Nuyken, H. Becker, K. Meerholz, *Nature* **2003**, *421*, 829.
[13] X. Jiang, S. Liu, M. S. Liu, H. Ma, A. K.-Y. Jen, *Appl. Phys. Lett.* **2000**, *76*, 2985.
[14] X. Gong, D. Moses, A. J. Heeger, S. Liu, A. K.-Y. Jen, *Appl. Phys. Lett.* **2003**, *83*, 183.
[15] W. Ma, P. K. Iyer, X. Gong, B. Lin, D. Moses, G. C. Bazan, A. J. Heeger, *Adv. Mater.* **2005**, *17*, 274.
[16] S. Sax, G. Mauthner, T. Piok, S. Pradhan, U. Scherf, E. J. W. List, *Org. Electron.* **2007**, *8*, 791.
[17] H.-G. Nothofer, PhD Thesis (ISBN 3-89722-668-5), University of Potsdam, Logos Verlag, Berlin **2001**.
[18] J. Jacob, J. Zhang, A. C. Grimsdale, K. Müllen, M. Gaal, E. J. W. List, *Macromolecules* **2003**, *36*, 8240.
[19] U. Scherf, E. J. W. List, *Adv. Mater.* **2002**, *14*, 477.
[20] Gaussian 03, Revision C.02, M. J. Frisch, G. W. Trucks, H. B. Schlegel, G. E. Scuseria, M. A. Robb, J. R. Cheeseman, J. A. Montgomery, Jr., T. Vreven, K. N. Kudin, J. C. Burant, J. M. Millam, S. S. Iyengar, J. Tomasi, V. Barone, B. Mennucci, M. Cossi, G. Scalmani, N. Rega, G. A. Petersson, H. Nakatsuji, M. Hada, M. Ehara, K. Toyota, R. Fukuda, J. Hasegawa, M. Ishida, T. Nakajima, Y. Honda, O. Kitao, H. Nakai, M. Klene, X. Li, J. E. Knox, H. P. Hratchian, J. B. Cross, C. Adamo, J. Jaramillo, R. Gomperts, R. E. Stratmann, O. Yazyev, A. J. Austin, R. Cammi, C. Pomelli, J. W. Ochterski, P. Y. Ayala, K. Morokuma, G. A. Voth, P. Salvador, J. J. Dannenberg, V. G. Zakrzewski, S. Dapprich, A. D. Daniels, M. C. Strain, O. Farkas, D. K. Malick, A. D. Rabuck, K. Raghavachari, J. B. Foresman, J. V. Ortiz, Q. Cui, A. G. Baboul, S. Clifford, J. Cioslowski, B. B. Stefanov, G. Liu, A. Liashenko, P. Piskorz, I. Komaromi, R. L. Martin, D. J. Fox, T. Keith, M. A. Al-Laham, C. Y. Peng, A. Nanayakkara, M. Challacombe, P. M. W. Gill, B. Johnson, W. Chen, M. W. Wong, C. Gonzalez, J. A. Pople, Gaussian, Inc., Wallingford, CT **2004**.
[21] M. J. S. Dewar, E. G. Zoebitsch, E. F. Healy, *J. Am. Chem. Soc.* **1985**, *107*, 3902.
[22] A. D. Becke, *J. Chem. Phys.* **1993**, *98*, 5648.
[23] P. J. Brewer, J. Huang, P. A. Lane, A. J. deMello, D. D. C. Bradley, J. C. de Mello, *Phys. Rev. B* **2006**, *74*, 115202.
[24] T. Woundenbergh, P. W. M. Blom, J. N. Huiberts, *Appl. Phys. Lett.* **2003**, *82*, 985.
[25] P. J. Brewer, P. A. Lane, J. Huang, A. J. deMello, D. D. C. Bradley, J. C. de Mello, *Phys. Rev. B* **2005**, *71*, 205209.
[26] A. van Dijken, J. A. M. J. Bastiaansen, N. M. M. Kiggen, B. M. W. Langeveld, C. Rothe, A. Monkman, I. Bach, P. Stössl, K. Brunner, *J. Am. Chem. Soc.* **2004**, *126*, 7718.
[27] J. Pina, J. S. de Melo, H. D. Burrows, A. P. Monkman, S. Navaratnam, *Chem. Phys. Lett.* **2004**, *400*, 441.
[28] S. Sax, N. Rugen-Penkalla, A. Neuhold, S. Schuh, E. Zojer, E. J. W. List, K. Müllen, unpublished.

Final page numbers not assigned